

See discussions, stats, and author profiles for this publication at: <https://www.researchgate.net/publication/231648242>

# Light-Triggered Conductance Switching in Single-Molecule Dihydroazulene/Vinylheptafulvene Junctions

ARTICLE *in* THE JOURNAL OF PHYSICAL CHEMISTRY C · AUGUST 2011

Impact Factor: 4.77 · DOI: 10.1021/jp205638b

CITATIONS

25

READS

39

6 AUTHORS, INCLUDING:



**Samuel Lara-Avila**

Chalmers University of Technology

49 PUBLICATIONS 749 CITATIONS

SEE PROFILE



**Andrey V Danilov**

Chalmers University of Technology

36 PUBLICATIONS 967 CITATIONS

SEE PROFILE



**Sergey Kubatkin**

Chalmers University of Technology

106 PUBLICATIONS 1,820 CITATIONS

SEE PROFILE



**Mogens Brøndsted Nielsen**

University of Copenhagen

132 PUBLICATIONS 2,079 CITATIONS

SEE PROFILE

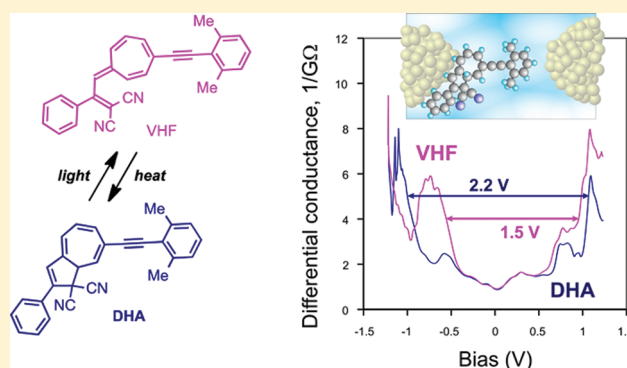
# Light-Triggered Conductance Switching in Single-Molecule Dihydroazulene/Vinylheptafulvene Junctions

Samuel Lara-Avila,<sup>†</sup> Andrey V. Danilov,<sup>\*,†</sup> Sergey E. Kubatkin,<sup>†</sup> Søren Lindbæk Broman,<sup>‡</sup> Christian Richard Parker,<sup>‡</sup> and Mogens Brøndsted Nielsen<sup>\*,‡</sup>

<sup>†</sup>Department of Microtechnology and Nanoscience, Chalmers University of Technology, Kemivägen 9, S-41296 Göteborg, Sweden

<sup>‡</sup>Department of Chemistry, University of Copenhagen, Universitetsparken 5, DK-2100 Copenhagen Ø, Denmark

**ABSTRACT:** Derivatives of 1,1-dicyano-1,8a-dihydroazulene (DHA) undergo light-induced ring-opening to a corresponding vinylheptafulvene (VHF), which in turn is thermally reverted to DHA. Here we have fabricated single-molecule DHA/VHF junctions and measured light-triggered conductance switching of these junctions. The DHA/VHF system studied includes a substituent group at the seven-membered ring. Light-induced conversion of this DHA to VHF in the junction is supported by a reduced tunnelling gap in tunnelling density of states. In fact, the reduced tunnelling gap corresponds to the reduced HOMO–LUMO gap of VHF relative to that of DHA as measured by absorption spectroscopy and electrochemistry. For this comparison, electrochemical measurements were performed on both the parent DHA/VHF system and the functionalized system that was subject to transport measurements. In one junction, it was possible to switch back and forth between DHA and VHF three times, the forward reaction being induced by light and the back-reaction occurring after waiting a period of time.



## INTRODUCTION

The design of molecular switches that change their single-molecule conductivity by an external stimulus is important for the development of functional molecular electronics devices.<sup>1</sup> Therefore, conventional computing operations can be performed by a single molecule working as a transistor or a logical switch. Light provides a particularly attractive stimulus for triggering conductivity changes.<sup>2</sup> The two most studied photoswitches in single-molecule molecular electronics are derivatives of dithienylethene<sup>3–6</sup> and azobenzene.<sup>7–9</sup> In solution, the first class of molecules is switched by light between an open and closed form, whereas the second class undergoes light-induced *trans*–*cis* isomerizations. Yet, a molecule may lose its photoswitching ability when connected to an electrode as strong electronic coupling to the metal may lead to quenching of the excited state of the photoswitch. Therefore, when adhered to electrodes, both the nature and position of the anchoring groups to the electrodes were found to be crucial for achieving either unidirectional<sup>3</sup> or bidirectional switching of dithienylethene molecules.<sup>4,5</sup> Calculations have revealed that decoupling via a cross-conjugated pathway between the switch and the anchoring groups or the internal rotational degree of freedom can account for reversible, that is, bidirectional, switching.<sup>6</sup> The geometrical change accompanying the *trans*–*cis* isomerizations of azobenzenes has been studied at surfaces by both STM<sup>7</sup> and a Hg drop electrode,<sup>8</sup> and calculations have revealed that the *trans*-azobenzene conducts better than the *cis*-azobenzene.<sup>9</sup>

In this Article, we present a system that analogous to the dithienylethenes undergoes a significant structural change upon irradiation, namely, the dihydroazulene (DHA)/vinylheptafulvene (VHF) system introduced by Daub and coworkers<sup>10</sup> in 1984. DHA **1** exhibits an absorption maximum at 353 nm in acetonitrile, and when irradiated at this wavelength it undergoes a ring-opening reaction to form the VHF **2** in its *s*-cis conformation (Scheme 1), with a quantum yield of 0.55.<sup>11</sup> The VHF exhibits a significantly red-shifted absorption maximum ( $\lambda_{\text{max}}$  470 nm in MeCN) reflecting the significant structural change of the molecule after ring-opening. Femtosecond spectroscopy on a related DHA (with a cyano group at the para position of the phenyl) showed that the ring-opening takes place within 1.2 ps on the DHA–VHF  $S_1$  potential energy surface.<sup>12</sup> It is followed by the internal conversion from VHF  $S_1$  to VHF  $S_0$  in 13 ps. The *s*-cis conformer is in equilibrium with its more stable *s*-trans conformer (Scheme 1). However, VHF is returned to DHA thermally, which has to proceed via the *s*-cis conformation. We have recently shown that the absorption maximum of the VHF can be strongly tuned by substituent groups.<sup>13–15</sup> For this reason and owing to the large difference in HOMO–LUMO gaps between DHA and VHF it is attractive to employ this system as a molecular switch for molecular electronics.

Received: June 16, 2011

Revised: August 13, 2011

Published: August 15, 2011

Scheme 1

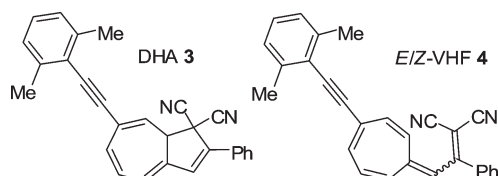
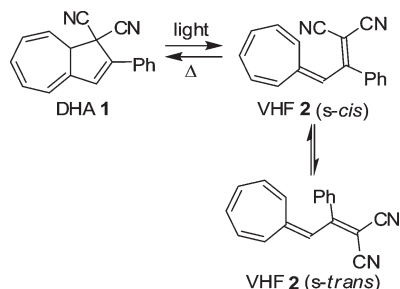


Figure 1

Our experimental technique for fabricating a single-molecule junction relies on the molecule being evaporated onto a substrate with prefabricated nanogap between silver electrodes (Experimental Methods); the same technique was previously employed for studies on oligo(phenylenevinylene)s<sup>16,17</sup> and fullerene-based<sup>18,19</sup> and anthraquinone switches.<sup>20</sup> The main advantage of our method is that no wet chemistry is involved in fabrication; the electrodes are deposited, and the molecule is sublimated and trapped in nanogap in the same vacuum cycle. This ensures that electrodes are perfectly clean, and there is no contamination, which can be mistaken for the molecule under study. Obviously, this method imposes some constraints on the molecule to be used: a suitable molecule must sublime without decomposition and should not be too volatile at room temperature.

We chose to investigate the DHA/VHF system 3/4,<sup>14</sup> incorporating an arylethynyl substituent in the seven-membered ring (Figure 1). Because of the higher molecular weight of 3 relative to 1, the sublimation temperature is increased to 160 °C so that the vapor pressure at room temperature is negligible. Thiol anchoring groups at the ends of the molecule were deliberately avoided to decrease coupling to the electrodes. For comparison of DHA/VHF transport gaps, we also subjected the compounds to an electrochemical study in solution, providing an estimate of the difference in HOMO–LUMO gap energy between the two isomers.

## RESULTS AND DISCUSSION

**Optical Properties.** The UV–vis absorption properties of 1–4 were previously reported,<sup>11,14</sup> but the results are included here for convenience. Therefore, it is relevant to compare the HOMO–LUMO gap obtained from conductance measurements to the corresponding optical as well as electrochemical ones (vide infra). The UV–vis spectra of 1–4 are shown in Figure 2. The longest wavelength absorption maximum of VHF 2 ( $\lambda_{\text{max}}$  470 nm, 2.64 eV) in acetonitrile was significantly red-shifted relative to that of DHA 1 (353 nm, 3.51 eV). DHA 3 exhibited an absorption maximum at 354 nm (3.50 eV) in acetonitrile, that is, a value close to that of 1 and was converted

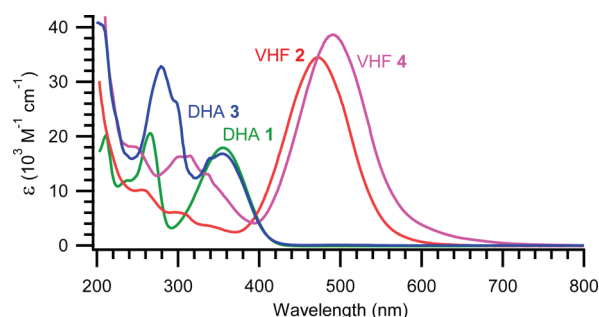


Figure 2. UV–vis absorption spectra of 1 (green curve), 2 (red curve), 3 (blue curve), and 4 (pink curve) in acetonitrile.

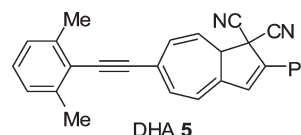
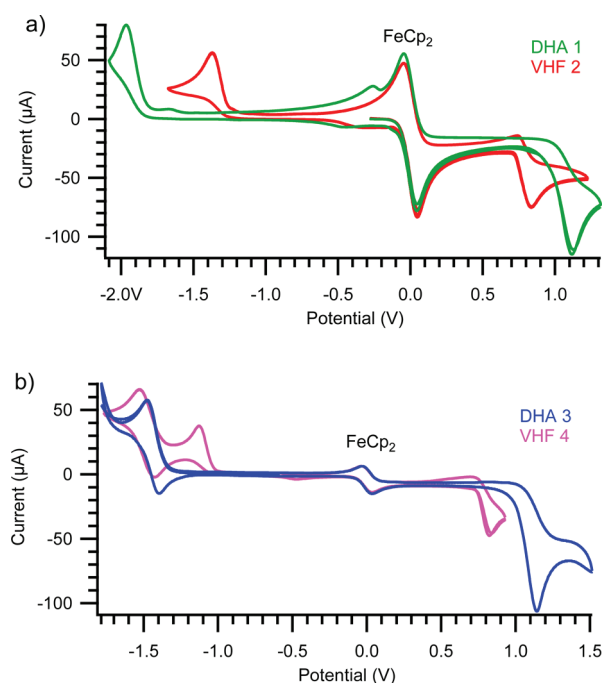


Figure 3

by irradiation to the VHF 4 (E/Z mixture) absorbing in acetonitrile at  $\lambda_{\text{max}}$  490 nm (2.53 eV).<sup>14</sup> From the spectra, we estimate the following absorption onsets: ca. 415 nm (2.99 eV) for 1 and 3, ca. 555 nm (2.23 eV) for 2, and ca. 580 nm (2.14 eV) for 4 (in each case the intercept value of the  $x$  axis by the tangent of the absorption curve). Accordingly, the differences in HOMO–LUMO gaps become 0.76 (1/2) and 0.85 eV (3/4). The thermal ring-closure of VHF 4 gave in cyclohexane the original DHA 3, whereas a mixture of 3 and the isomer 5 (Figure 3) was generated in a polar solvent like acetonitrile. Any ring-opening/closure cycles in polar solvents were therefore avoided before studying DHA 3 in a device.

**Electrochemistry.** To gain a better insight into the redox properties of the system, DHA 1/VHF 2 and DHA 3/VHF 4 were studied by cyclic voltammetry (in acetonitrile and in the presence of ferrocene as reference compound). The cyclic voltammograms (CVs) are revealed in Figure 4. DHA 1 underwent an irreversible oxidation event at +1.09 V versus  $\text{FcP}_2/[\text{FcP}_2]^+$  (0.00 V). Upon sweeping back in the negative direction, a smaller reduction peak was observed at −0.24 V, which was presumably caused from a product formed at the irreversible oxidation event. The reduction of DHA gave an irreversible reduction at −1.95 V. We note that scanning to more negative potentials gave further reduction peaks (not shown). VHF 2 showed a partially reversible oxidation ( $i_c/i_a = 0.2$ ) at +0.78 V. There was an irreversible reduction at −1.34 V, which was followed by a reversible reduction at −2.45 V (not shown). The first reduction potential of the VHF 2 was close to that reported for  $\text{PhCH}=\text{C}(\text{CN})_2$ : −1.444 V versus  $\text{FcP}_2/[\text{FcP}_2]^+$  in MeCN.<sup>21</sup> In comparison, benzonitrile was reduced at −2.7 V in MeCN.<sup>22</sup> While being a weaker acceptor than the VHF, the DHA was still more readily reduced than benzonitrile, and the first electron is most likely added to the conjugated system rather than to one of the cyano groups. The more ready reduction of VHF derivatives than corresponding DHA derivatives was previously exploited in photoelectrochemical experiments (photomodulation amperometry) by Daub and coworkers.<sup>23,24</sup> Therefore, a cathodic current response was observed upon irradiation of a DHA solution subjected to a bias voltage that was in between the reduction waves of the DHA and VHF species.



**Figure 4.** Cyclic voltammogram of (a) DHA 1 (green trace) and VHF 2 (red trace) and (b) DHA 3 (blue trace) and VHF 4 (pink trace) with  $\text{FeCp}_2$  (ferrocene) as an internal reference ( $\text{FeCp}_2/[\text{FeCp}_2]^+$ ;  $E = 0.00$  V) scanned at 100 mV/s. Solvent: MeCN containing 0.1 M  $[\text{NBu}_4]\text{PF}_6$  as the supporting electrolyte. Working electrode: glassy carbon; reference electrode: silver; counter electrode: platinum. The current measured for VHF 4 was scaled by a factor of 1000 in the CV shown.

Oxidations and reductions of DHA and VHF are likely accompanied by chemical reactions, as also previously reported,<sup>25,26</sup> and a more detailed electrochemical study of the DHA/VHF system 1/2 is currently being conducted and will be described elsewhere.

Addition of the aryethynyl group to the seven-membered ring increases the conjugation and adds a mildly electron withdrawing group to the molecule, which gave a noticeable change in the electrochemical properties of 3/4 compared with 1/2. DHA 3 underwent an irreversible oxidation at +1.14 V, which is similar to that of 1. However, unlike 1, this first oxidation peak appears to be twice as intense as the first reduction peak. (See Figure 4b.) The first reduction of 3 occurring at −1.44 V was easier by ~0.5 V than for 1 and more reversible ( $i_a/i_c = 0.85$ ). Further scanning in the negative direction gave more irreversible reductions (not shown). The first oxidation event of the VHF 4 was similar to that of 2 at +0.77 V but was slightly more reversible ( $i_c/i_a = 0.4$ ). The first reduction event of VHF 4 occurred irreversibly at −1.13 V, and the compound is hence ~0.2 V easier to reduce than 2. There was a second reduction event at −1.48 V, which appeared to be reversible. Two irreversible reduction events were observed at a more negative potential (not shown). It must also be noted that unlike in the parent system, prolonged exposure (a further 20 min after the initial 20 min for switching 3 to 4) to the UV lamp (365 nm) caused the appearance of even more redox events. This suggested that there was another species formed, potentially from a photoinduced chemical reaction, so care must be taken with the UV exposure time.

It was clear for both systems that the VHF was easier to oxidize and reduce than its corresponding DHA. From the first oxidation onsets (1: +0.97 V, 2: +0.72 V, 3: +1.01 V, 4: +0.74 V) and first

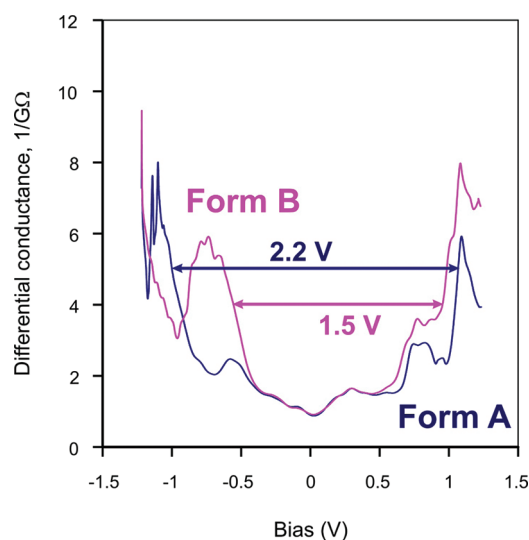


**Figure 5.** Differential conductance plot for single-molecule DHA junction revealing the tunnelling density of states before (Form A) and after (Form B) light-induced switching.

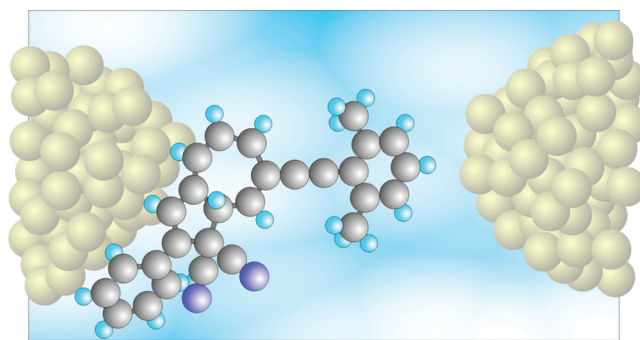


**Figure 6.** Schematic representation of the sample geometry. The DHA molecule is well-coupled to one electrode and separated from the other by a tunnelling gap.

reduction onsets (1: −1.83 V, 2: −1.25 V, 3: −1.36 V, 4: −1.03 V), we obtain electrochemical HOMO–LUMO gaps of 2.80 (DHA 1), 1.97 (VHF 2), 2.37 (DHA 3), and 1.77 eV (VHF 4). Therefore, the HOMO–LUMO gap was reduced by 0.83 eV for 2 relative to 1 and by 0.60 eV for 4 relative to 3. Whereas the optical and electrochemical HOMO–LUMO gap difference between VHF and DHA matches quite well for the parent system 1/2, there was a small deviation of 0.25 eV for 3/4. It should be emphasized, however, that in the estimation of the electrochemical energy gaps, we have ignored the irreversibility due to chemical follow-up reactions; the values provided above are hence only rough estimates and should be interpreted with some care.

**Conductance Measurements.** Following the fabrication procedure as described in the Experimental Methods (and described in more detail in previous work<sup>16–20,27,28</sup> including detailed nano-gap characterization without the presence of molecules<sup>27,28</sup>), we have fabricated four independent single-molecule DHA 3 junctions. All four samples demonstrated reproducible tunnelling spectra in the original state, that is, before the light was shined on the junction (see an exemplary differential conductance plot for Form A in Figure 5), with the transport gap being in the range of 2.1 to 2.4 eV.



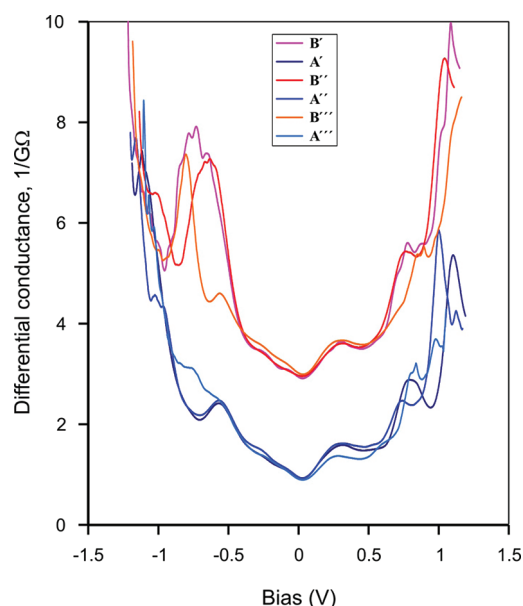


**Figure 7.** Multiple reversible switching between forms A and B in one of the samples measured. The curves for form B are offset for clarity.<sup>30</sup>

**Table 1. Summary of HOMO–LUMO Gaps (electronvolts) Estimated from Solution and Junction Studies**

| molecule | spectroscopy | cyclic voltammetry | junction    |
|----------|--------------|--------------------|-------------|
| DHA 1    | 2.99         | 2.80               |             |
| VHF 2    | 2.23         | 1.97               |             |
| DHA 3    | 2.99         | 2.37               | 2.1 to 2.4  |
| VHF 4    | 2.14         | 1.77               | 1.5 to 1.75 |

None of the four samples revealed gate-induced conductance modulation or Coulomb blockade effects. This implies that in all samples the molecule was well coupled to at least one electrode. For different samples the sample resistance varied from 20 MΩ to 20 GΩ, which means that in all junctions the molecule was separated from the other electrode by a tunnelling gap, as depicted in Figure 6. This type of asymmetric sample topology usually is the result of our fabrication procedure.<sup>16–20</sup> The width of the tunnelling gap is not under experimental control and can vary from sample to sample so that the overall sample conductance is not a molecular-specific characteristic; it is tunnelling spectroscopy data that identify a specific molecule.

To study the effects of light irradiation, we fitted the vacuum chamber with a UV diode with maximum output at 355 nm. As it was stated above, before shining light, the samples were checked for the absence of the gate effect. Typical gate measurements (S12 *I*–*V* curves for different gate voltages) take ~2 h for 20 MΩ samples and ~12 h for 20 GΩ samples. No spontaneous switching in the sample conductance was observed during this time interval.

One sample did not respond to the light; in three other samples, turning the UV light on triggered a distinct switching event after irradiation for about 10–20 min. Once a single switching event had happened, further irradiation had no effect. The switched sample showed a reduction of transport gap in tunnelling density of states (Figure 5). Turning the light off and waiting for a few hours while measuring an (reproducible) *I*–*V* curve,<sup>29</sup> we

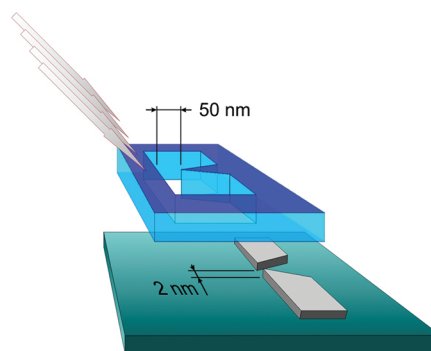
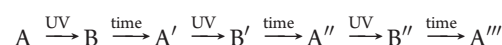


**Figure 8.** Tuning the nanogap width by oblique deposition. The proper inclination could be found by a few in situ test depositions with incrementally reduced tilt.

managed to reset a sample presented in Figure 5 back to original Form A. In total, we recorded the following chain of transitions for this sample (Figure 7)



In the other sample, the UV light triggered a single  $A \rightarrow B$  transition with differential conductance after switching similar to Form B in Figure 5, but we did not manage to reset this sample back to Form A. Finally, one more sample was burned as a result of a single light-triggered switching.

## DISCUSSION

The observed reduction of transport gap in tunnelling density of states by 0.7 to 1 eV as a result of  $A \rightarrow B$  transition in molecular junctions matches the reduced HOMO–LUMO gap of VHF 4 relative to that of DHA 3 determined by optical and electrochemical means, ca. 0.85 and 0.60 eV, respectively. We can, therefore, reasonably identify the A and B forms for molecule in the nanogap as corresponding to the DHA 3 and VHF 4 configurations, respectively. The general renormalization of HOMO–LUMO gap from 2.99 eV (optical) for DHA in solution down to 2.2 eV for molecule placed in nanogap is quite common and understood.<sup>16,17,31,32</sup>

Another crucial observation, which identifies DHA/VHF as a molecular junction kernel is, of course, the photosensitivity. We shall now estimate the expected switching time for our setup and compare it with the experimental results. The UV LED had emitting power of 550 μW; the light was directed to a spot about 15 mm in diameter at the sample plane, which corresponds to the light flux of ~5 photons per square nanometer per second. A molar light absorptivity of ca. 17 000 M<sup>−1</sup> cm<sup>−1</sup>, as measured in solution (Figure 2), translates into a cross-section for photo-induced reaction of ~0.003 nm<sup>2</sup>, which corresponds to the expected switching time of ~1 min. The experimentally observed switching time was about 10–20 min. Although we only have limited statistics (six switching events were recorded), the cross-section for photoswitching seems to be one order of magnitude lower for molecule in a junction as compared with DHA in solution. We attribute this to a fast relaxation of electronic excitations mediated by exchange with electrodes. Indeed, the peaks on differential conductance plot are ~100 meV wide (Figure 5), which translates into electron residence time of ~40 fs. This means that an excited electron can escape to the leads much faster than the time 1.2 ps needed for the ring-

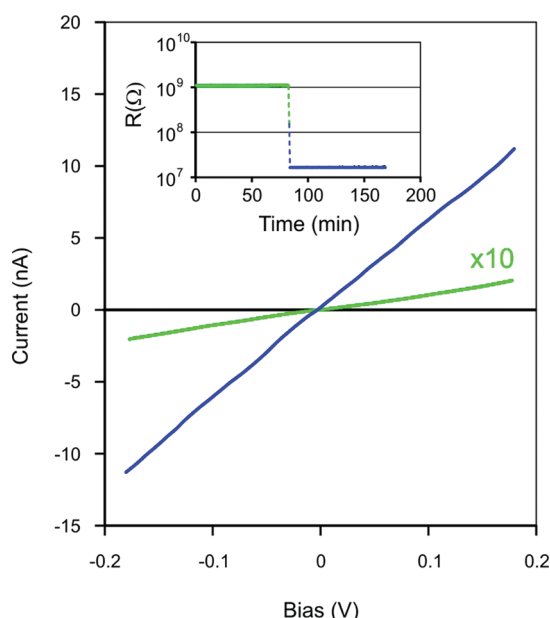


**Figure 9.** Main plot: sample  $I(V)$  curves before (green curve) and after (blue curve) the molecule was caught. The former curve is up-scaled 10 times for clarity. Inset: sample conductance versus time during annealing process. The temperature was slowly raised from 4 to 50 K when a single conductance switching event happened and the sample was cooled back to 4 K.

opening (measured for a related system<sup>33</sup>), and only a small fraction of photoexcited electrons resides on the molecule long enough to trigger the conversion.

Finally, the experiment shows that not all single-molecule junctions demonstrate exactly the same switching properties: although most junctions were photosensitive, some were not. In a similar way, although most samples were quenched after photoswitching in form B, some samples could be reset back to form A. We attribute this to a different switching barrier for different samples, which is not surprising having in mind that the switching may be accompanied by an *s-cis* to *s-trans* conformational change. The barrier for this rotation should depend on the exact placement/orientation of the molecule in nanogap, which is not under experimental control. However, we like to stress that the HOMO–LUMO structure for both DHA and VHF forms is quite reproducible; that is, counting all measured samples, reproducible tunnelling spectra were registered seven times for the DHA form and four times for the VHF form. This implies that the chemical identity of both the DHA and the VHF forms is not disturbed by the solid-state environment; it is only the coupling of LUMO to the electrode (and possibly the switching barrier between the two forms) that varies from sample to sample.

## CONCLUSIONS

In conclusion, we have fabricated the first single-molecule junction of a derivative of the DHA photoswitch and measured reproducible tunnelling spectra. The junction was found to undergo light-triggered conductance switching, corroborating that the DHA photoswitch molecule was indeed incorporated in the junction. Moreover, the light-induced single-molecule junction is characterized by a reduced transport gap in tunnelling density of states, which strongly supports that the new junction contained the ring-opened VHF derivative because this compound has a reduced HOMO–LUMO gap relative to that of the

original DHA according to both absorption spectroscopy and cyclic voltammetry studies in solution (Table 1).

For one light-exposed sample, it was possible to reset the junction to the original DHA after waiting a period of time, and it was possible to do a total of three switching cycles with this sample. The thermal ring-closure of VHF requires the molecule to be in its *s-cis* conformation, and the failure of the other samples to reset to DHA may be the result of a conformational change to the more favorable *s-trans* conformer at the surface.

## EXPERIMENTAL METHODS

**Electrochemistry.** Electrochemical samples (1 mM) were dissolved in MeCN containing 0.1 M  $[\text{NBu}_4]\text{PF}_6$  as the supporting electrolyte. Electrodes: glassy carbon working, silver reference and platinum counter. When measuring DHA, the electrochemical cell was covered in aluminum foil to prevent light from entering the DHA solution. The VHF was formed by removing the aluminum foil from around the cell and irradiating the solution with a long wavelength UV (365 nm) lamp, turning the color of the solution from yellow to dark red. Complete conversion was observed within 20 min.

**Sample Fabrication.** A planar gate electrode made of aluminum metal covered with aluminum oxide (5 nm thick) was prepared on a chip of oxidized silicon. The shadow mask for deposition of source-drain electrodes was defined by E-beam lithography on top of the gate electrode. The sample chip was then introduced to a vacuum chamber completely immersed into liquid He. The electrodes were deposited through a mask by condensing silver vapor on the substrate held at 4.2 K. The mask had an opening, which is  $\sim 50$  nm wide in the narrowest place, as shown in Figure 8. To reduce the nanogap width down to desired  $\sim 2$  nm, we used deposition at an angle that effectively squeezes the opening in resist, as illustrated in Figure 8. The proper tilt angle was found by a few *in situ* depositions while incrementing the tilt and checking for conductance.

In a subsequent step, the DHA molecules were sublimated through the same mask in a submonolayer coverage ( $<1\%$ ). At 4 K, the molecules are stuck at the sites where they initially land on the substrate. A submonolayer of deposited molecules leaves the  $I$ – $V$  characteristic of the gap intact, indicating that no molecules have evaporated directly into the gap. To catch the molecule, we raised the temperature to 30–60 K to activate the surface diffusion of DHA molecules. At some moment the sample resistance, in a single event, drops from  $\sim 10^9$  to  $10^{10}$  Ω down to  $\sim 10^8$  to  $10^7$  Ω, indicating the trapping of a single molecule in the nanogap. Exemplary data for one of the samples studied are presented in Figure 9. Once the molecule was trapped, the sample was cooled back to a base temperature of 4 K.

## AUTHOR INFORMATION

### Corresponding Author

\*E-mail: andrey.danilov@chalmers.se (A.V.D.); mbn@kiku.dk (M.B.N.).

## ACKNOWLEDGMENT

The research leading to these results has received funding from the European Community's Seventh Framework Programme (FP7/2007-2013) under the grant agreement "SINGLE" no 213609. The Villum Kann Rasmussen Foundation is

also gratefully acknowledged. We thank Prof. Ole Hammerich (University of Copenhagen) and Prof. Jörg Daub (University of Regensburg) for helpful discussions on the electrochemistry.

## REFERENCES

- (1) Weibel, N.; Grunder, S.; Mayor, M. *Org. Biomol. Chem.* **2007**, *5*, 2343–2353.
- (2) Tsujioka, T.; Irie, M. *J. Photochem. Photobiol., C* **2010**, *11*, 1–14.
- (3) Dulic, D.; van der Molen, S. J.; Kudernac, T.; Jonkman, H. T.; de Jong, J. J. D.; Bowden, T. N.; van Esch, J.; Feringa, B. L.; van Wees, B. J. *Phys. Rev. Lett.* **2003**, *91*, 207402.
- (4) Katsonis, N.; Kudernac, T.; Walko, M.; van der Molen, S. J.; van Wees, B. J.; Feringa, B. L. *Adv. Mater.* **2006**, *18*, 1397–1400.
- (5) van der Molen, S. J.; Liao, J.; Kudernac, T.; Augustsson, J. S.; Bernard, L.; Calame, M.; van Wees, B. J.; Feringa, B. L.; Schönenberger, C. *Nano Lett.* **2009**, *9*, 76–80.
- (6) Zhuang, M.; Ernzerhof, M. *J. Chem. Phys.* **2009**, *130*, 114704.
- (7) Kumar, A. S.; Ye, T.; Takami, T.; Yu, B.-C.; Flatt, A. K.; Tour, J. M.; Weiss, P. S. *Nano Lett.* **2008**, *8*, 1644–1648.
- (8) Ferri, V.; Elbing, M.; Pace, G.; Dickey, M. D.; Zharnikov, M.; Samori, P.; Mayor, M.; Rampi, M. A. *Angew. Chem., Int. Ed.* **2008**, *47*, 3407–3409.
- (9) Zhang, C.; He, Y.; Cheng, H.-P.; Xue, Y.; Ratner, M. A.; Zhang, X.-G.; Krstic, P. *Phys. Rev. B* **2006**, *73*, 125445.
- (10) Daub, J.; Knöchel, T.; Mannschreck, A. *Angew. Chem., Int. Ed. Engl.* **1984**, *23*, 960–961.
- (11) Görner, H.; Fischer, C.; Gierisch, S.; Daub, J. *J. Phys. Chem.* **1993**, *97*, 4110–4117.
- (12) De Waele, V.; Beutter, M.; Schmidhammer, U.; Riedle, E.; Daub, J. *Chem. Phys. Lett.* **2004**, *390*, 328–334.
- (13) Petersen, M. Å.; Broman, S. L.; Kadziola, A.; Kilså, K.; Nielsen, M. B. *Eur. J. Org. Chem.* **2009**, 2733–2736.
- (14) Broman, S. L.; Petersen, M. Å.; Tortzen, C.; Kadziola, A.; Kilså, K.; Nielsen, M. B. *J. Am. Chem. Soc.* **2010**, *132*, 9165–9174.
- (15) Petersen, M. Å.; Broman, S. L.; Kilså, K.; Kadziola, A.; Nielsen, M. B. *Eur. J. Org. Chem.* **2011**, 1033–1039.
- (16) Kubatkin, S.; Danilov, A.; Hjort, M.; Cornil, J.; Brédas, J.-L.; Stuhr-Hansen, N.; Hedegård, P.; Bjørnholm, T. *Nature* **2003**, *425*, 698–701.
- (17) Kubatkin, S.; Danilov, A.; Hjort, M.; Cornil, J.; Brédas, J.-L.; Stuhr-Hansen, N.; Hedegård, P.; Bjørnholm, T. *Curr. Appl. Phys.* **2004**, *4*, 554–558.
- (18) Danilov, A. V.; Kubatkin, S. E.; Kafanov, S. G.; Bjørnholm, T. *Faraday Discuss.* **2006**, *131*, 337–345.
- (19) Danilov, A. V.; Hedegård, P.; Golubev, D. S.; Bjørnholm, T.; Kubatkin, S. E. *Nano Lett.* **2008**, *8*, 2393–2398.
- (20) Lara-Avila, S.; Danilov, A.; Geskin, V.; Bouzakraoui, S.; Kubatkin, S.; Cornil, J.; Bjørnholm, T. *J. Phys. Chem. C* **2010**, *114*, 20686–20695.
- (21) Zhu, X.-Q.; Zhang, M.; Liu, Q.-Y.; Wang, X.-X.; Zhang, J.-Y.; Cheng, J.-P. *Angew. Chem., Int. Ed.* **2006**, *45*, 3954–3957.
- (22) Uosaki, K.; Murakoshi, K.; Kita, H. *J. Phys. Chem.* **1991**, *95*, 779–783.
- (23) Daub, J.; Salbeck, J.; Knöchel, T.; Fischer, C.; Kunkely, H.; Rapp, K. M. *Angew. Chem., Int. Ed. Engl.* **1989**, *28*, 1494–1496.
- (24) Daub, J.; Fischer, C.; Salbeck, J.; Ulrich, K. *Adv. Mater.* **1990**, *2*, 366–369.
- (25) Spreitzer, H.; Daub, J. *Chem.—Eur. J.* **1996**, *2*, 1150–1158.
- (26) Mrozek, T.; Ajayaghosh, A.; Daub, J. In *Molecular Switches*; Feringa, B. L., Ed.; Wiley-VCH: Weinheim, Germany, 2001; pp 63–106.
- (27) Kubatkin, S. E.; Danilov, A. V.; Olin, H.; Claeson, T. *J. Low Temp. Phys.* **2000**, *118*, 307–316.
- (28) Danilov, A. V.; Golubev, D. S.; Kubatkin, S. E. *Phys. Rev. B* **2002**, *65*, 1253121–1253129.
- (29) We also tried to promote the reverse switching by applying a high gate voltage. Neither gate nor bias voltages seemed to facilitate  $B \rightarrow A$  switching.
- (30) The initial state A was measured up to a maximum bias of 700 mV only and therefore is not shown in Figure 7.
- (31) Kaasbjerg, K.; Flensberg, K. *Nano Lett.* **2008**, *8*, 3809–3814.
- (32) Osorio, E. A.; O'Neill, K.; Stuhr-Hansen, N.; Nielsen, O. F.; Bjørnholm, T.; van der Zant, H. S. J. *Adv. Mater.* **2007**, *19*, 281–285.
- (33) When one electron moves from the excited state into electrode, the other one fills the ground-state level so that electroneutrality is, of course, never broken.